Translational Oncology
www.transonc.com

Volume 11 Number xx Month 2018 pp. 74–85 74

Cancer-Specific Inhibitory Effects of Genetically Engineered Stem Cells Expressing Cytosine Deaminase and Interferon-β Against Choriocarcinoma in Xenografted Metastatic Mouse Models

Gyu-Sik Kim[*], Jae-Rim Heo[*], Seung U. Kim[†] and Kyung-Chul Choi[*,‡]

[*]Laboratory of Biochemistry and Immunology, College of Veterinary Medicine, Chungbuk National University, Cheongju, Chungbuk, Republic of Korea; [†]Department of Medicine, Faculty of Medicine, University of British Columbia, Vancouver, British Columbia, Canada; [‡]Institute of Life Science and Bio-Engineering, TheraCell Bio & Science, Cheongju, Chungbuk, Republic of Korea

Abstract

Cancer treatments using stem cells expressing therapeutic genes have been identified for various types of cancers. In this study, we investigated inhibitory effects of HB1.F3.CD and HB1.F3.CD.IFN-β cells expressing *Escherichia coli* cytosine deaminase (CD) and human interferon-β (IFN-β) genes in intravenously (i.v.) injected mice with a metastasis model. In this treatment, pro-drug 5-fluorocytosine (5-FC) is converted to cytotoxic drug 5-fluorouracil by hNSCs expressing the CD gene, which inhibits DNA synthesis in cancer cells. Moreover, IFN-β induces apoptosis and reduces the growth of cancer cells. Upon MTT assay, proliferation of choriocarcinoma (JEG-3) cells decreased when co-cultured with hNSCs expressing CD and IFN-β genes. To confirm the cancer-tropic effect of these stem cells, chemoattractant factors (VEGF, CXCR4, and C-kit) secreted from JEG-3 cells were identified by polymerase chain reaction. hNSCs migrate toward JEG-3 cells due to ligand-receptor interactions of these factors. Accordingly, the migration capability of hNSCs toward JEG-3 cells was confirmed using an *in vitro* Trans-well assay, *in vivo* subcutaneously (s.c.) injected mice groups (xenograft model), and metastasis model. Intravenously injected hNSCs migrated freely to other organs when compared to s.c. injected hNSCs. Thus, we confirmed the inhibition of lung and ovarian metastasis of choriocarcinoma by i.v. injected HB1.F3.CD or HB1.F3.CD.IFN-β cells in the presence of 5-FC. Treatment of these stem cells also increased the survival rates of mice. In conclusion, this study showed that metastatic cancer was diminished by genetically engineered hNSCs and noncytotoxic drug 5-FC. This is the first report of the therapeutic potential of i.v. injected hNSCs in a metastasis model; therefore, the results indicate that this stem cell therapy can be used as an alternative novel tool to treat metastatic choriocarcinoma.

Translational Oncology (2018) 11, 74–85

Introduction

Choriocarcinoma is a rare malignant gestational trophoblastic disease that mainly occurs in women of reproductive age and is likely to spread to other organs [1,2]. Choriocarcinoma can be divided into gestational and nongestational choriocarcinoma. Gestational choriocarcinoma is mostly preceded by a hydatidiform mole and spontaneous abortion. Rarely, nongestational choriocarcinoma occurs in male gonadal organs [3]. Choriocarcinoma occurs about three to nine times more often in Asia than in Europe and North America [4]. This form of cancer is known as a metastatic tumor that has a poor clinical outcome when cancer cells are widely spread. Choriocarcinoma cancer cells are metastasized through hematogenous routes to the lungs, liver, brain, etc., although the most common site is the lungs [1,3,5]. Most choriocarcinomas have a significant therapeutic effect on chemotherapy. However, drugs commonly used for cancer

Address all correspondence to: Kyung-Chul Choi, DVM, PhD, Laboratory of Biochemistry and Immunology, College of Veterinary Medicine, Chungbuk National University, Cheongju, Chungbuk, 28644, Republic of Korea.
E-mail: kchoi@cbu.ac.kr
Received 21 July 2017; Revised 11 November 2017; Accepted 13 November 2017

1936-5233
https://doi.org/10.1016/j.tranon.2017.11.003

treatment have barriers such as drug resistance and side effects [6]. Furthermore, metastasis to other organs reduces the curable rate of chemotherapy [7]. Therefore, new strategies for the stable treatment of metastatic choriocarcinoma are needed.

Gene therapy that selectively targets cancer cells is an alternative to conventional therapies for effective treatment metastatic choriocarcinoma. Gene-directed enzyme prodrug therapy (GDEPT) is a noble method of cancer treatment that minimizes adverse effects [8]. This system selectively targets cancer cells using the bystander effect of a suicide enzyme that converts an inactive drug into an active one [9–11]. The representative system of GDEPT is CD/5-FC therapy, in which 5-fluorocytosine (5-FC) is converted to 5-fluorouracil (5-FU) by *Escherichia coli* cytosine deaminase (CD). This leads to suppression of DNA synthesis and apoptosis in tumor cells [12–15]. Interferon-β (IFN-β), a member of the type I interferons, blocks cell cycle progression in the S-phase [16]. High concentrations of IFN-β are known to inhibit viability of cancer cells *in vitro* but are limited *in vivo* due to problems caused by excessive toxicity [13,17]. Thus, it is necessary to identify efficient methods of cancer treatment through various vehicles for delivering therapeutic genes.

Human neural stem cells (hNSCs) are a suitable vehicle for cancer therapy that conveys anticancer genes to cancer cells [18,19]. Intravenously (i.v.) injected hNSCs have been shown to be especially effectively recruited to distant lesions [20]. Thus, we used immortalized HB1.F3 NSCs acquired from the telencephalon of a 15-week-old fetus, and retroviral vectors encoding the *v-myc* gene to immortalize HB1.F3 cells [21]. These cells were transduced to express anticancer genes. There are two types of cells. HB1.F3.CD cells expressed only CD gene, and HB1.F3.CD.IFN-β cells expressed both CD and IFN-β genes. Unlike conventional chemotherapy, stem cell therapy using these hNSCs can specifically diminish cancer cells [19,22–24], indicating that hNSCs have cancer-specific migration capability through interactions with various types of cancer cells that secrete chemoattractant factors [25]. This is a potentially powerful approach that can minimize the effects of drugs on normal tissues and effectively suppress cancer proliferation [26]. Several previous studies have reported that hNSCs expressing the therapeutic genes migrate to the tumor and impede tumor growth [9,27–29].

In this study, we verified that genetically engineered human NSCs are a potentially powerful approach to malignant choriocarcinoma treatment. Among the choriocarcinoma cell lines, JEG-3 cells, which have been shown to have high invasion ability, were used in the experiments [30]. We identified the migration ability of hNSCs by chemoattractant factors excreted from JEG-3 cells. Additionally, we observed changes in cell proliferation by CD/5-FC and IFN-β genes in the co-culture system of JEG-3 and hNSCs. Furthermore, we confirmed that HB1.F3.CD and HB1.F3.CD.IFN-β cells effectively diminished lung metastasis when i.v. injected in mice. Overall, we demonstrated the therapeutic efficacy of i.v. injected hNSCs in a lung metastasis mouse model for the first time.

Materials and Methods

Cell Culture and Media

Human placental choriocarcinoma cells (JEG-3) and normal human pulmonary epithelial cells (L-132) were purchased from the Korean Cell Line Bank (KCLB). L-132 cells were used as a control in migration assay [31]. Three types of genetically engineered human neural stem cells (hNSCs; HB1.F3, HB1.F3.CD, and HB1.F3.CD.IFN-β) were provided by Dr. Seung U. Kim (University of British Columbia) and used in this study. All cell lines were cultured in Dulbecco's modified Eagle's medium (DMEM; Hyclone Laboratories) supplemented with 10% (v/v) heat-inactivated fetal bovine serum (FBS; Hyclone Laboratories), 10 U/ml penicillin and 100 μg/ml streptomycin (Cellgro Mediatech), 10 mM HEPES (Invitrogen Life Technologies), and plasmocin as antimycoplasmal agents (Invivogene) at 37°C under 5% CO_2 and 95% air in a humidified cell incubator. The cells were trypsinized with 0.05% trypsin 0.02% EDTA (PAA Laboratories).

Reverse Transcription Polymerase Chain Reaction (PCR) Analysis

Total RNAs were isolated from HB1.F3.CD and HB1.F3.CD.IFN-β cells with TriZol Reagent (Invitrogen Life Technologies), after which M-MLV RT (iNtRON Biotechnology) was used for reverse transcription from 1 μg of mRNA to cDNA according to the manufacturer's protocols. *Escherichia coli* cytosine deaminase (CD) and human interferon-β (IFN- β) genes were amplified from hNSCs by PCR using each primer. In addition, chemoattractant factors including vascular endothelial growth factor (VEGF), vascular endothelial growth factor receptor (VEGFR), stromal cell–derived factor 1α (SDF-1α), stem cell factor (SCF), C-X-C chemokine receptor type 4 (CXCR4), and C-kit were amplified by PCR in JEG-3 and HB1.F3.CD.IFN-β cells. Human glyceraldehyde-3-phosphate dehydrogenase (GAPDH) was the internal control of this experiment. Samples were analyzed by electrophoresis on 1.5% agarose gel containing NEOgreen (NEO Science).

Migration Assay

To investigate the migration ability of hNSCs to human placental choriocarcinoma, a migration assay was performed using Trans-well chambers (8.0 μm pore; BD Biosciences). JEG-3 (1×10^5 cells/well) and L-132 (1×10^5) were seeded in a 24-well plate with 5% charcoal-dextran treated FBS phenol free DMEM. After incubation at 37°C for 24 hours, hNSCs (1×10^5 cells/well) were seeded in the upper chambers. The membranes of the upper chambers were precoated with fibronectin (250 μg/ml; Sigma-Aldrich). After incubation at 37°C for 18 hours, cells in the membrane were fixed with 3.7% formaldehyde solution (Sigma-Aldrich) for 10 minutes and then permeabilized with 100% methanol (Sigma-Aldrich) for 10 minutes. To count the cells, the membranes were dyed with crystal violet for 10 minutes. The migrated cells were then identified with an IX-73 Inverted Microscope (Olympus) and counted using the Cell Sense Dimension software (Olympus).

MTT Assay

JEG-3 cells (2000 cells/well) were seeded in 96-well plates to measure the cell viability of human choriocarcinoma by 5-FC and 5-FU treatment. Cells were cultured in phenol-free DMEM including 5% charcoal-dextran treated FBS, 1% HEPES, and 1% penicillin G and streptomycin. After incubation at 37°C for 24 hours, 5-FC and 5-FU (100, 200, 300, 400, and 500 μg/ml) diluted in PBS were treated for 3 days in wells containing JEG-3 cells. JEG-3 cells (1000 or 2000 cells/well) and hNSCs (1000 or 2000 or 4000 cells/well) were co-cultured to confirm the effects of hNSCs expressing CD and the IFN- β gene. After 24 hours, various concentrations of 5-FC (100, 200, 300, 400, and 500 μg/ml) diluted in PBS were treated for 3 days in wells. MTT solution (10 μl; 5 mg/ml) was added to all wells to confirm JEG-3 cell viability. Following incubation at 37°C for 4 hours, supernatants were removed, and 100 μl of dimethyl sulfoxide (99.0%) was added to all wells to solubilize formazan crystals. After

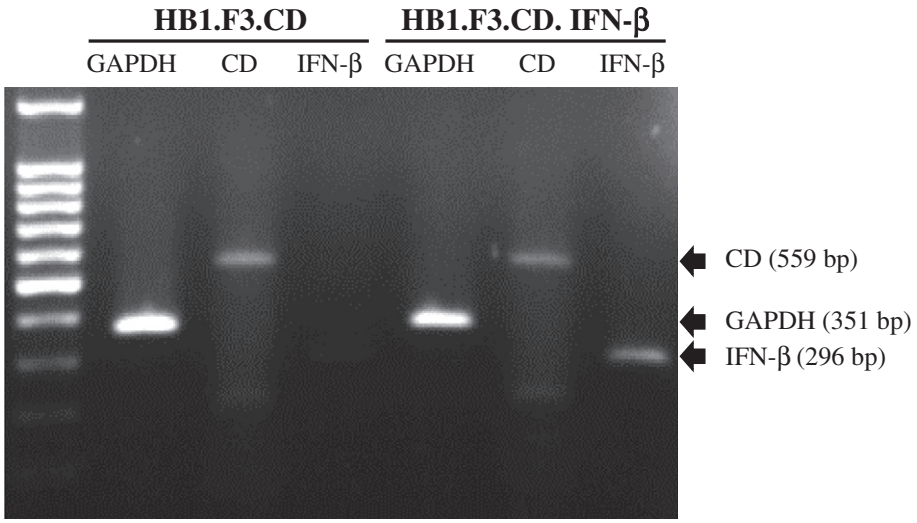

Figure 1. Presence of CD and/or IFN-β genes in genetically engineered hNSCs was confirmed by PCR. Expression of therapeutic genes was confirmed in HB1.F3.CD and HB1.F3.CD.IFN-β cells. cDNAs were amplified with PCR after total RNA extraction and cDNAs synthesis. These PCR products were separated by electrophoresis gel and confirmed by LuminoGraph II. GAPDH (351 bp) was used as the internal control for CD (559 bp) and IFN-β (296 bp) in each cell type.

shaking for 10 minutes, the optical densities were measured at 540 nm using an Epoch Microplate Spectrophotometer (BioTek). All assays were repeated at least three times.

Human Choriocarcinoma Xenograft and Metastasis Model in Athymic Nude Mice

Athymic nude mice (4-week-old females) were purchased from KOATECH. Experiments were conducted according to the protocol approved by the Chungbuk National University Institutional Animal Care and Use Committees (CBNUA-997-16-01). One week before the experiment, mice were acclimatized to the environment (24°C, 12-hour light/dark cycle). To generate xenograft models, CMFDA prestained JEG-3 cells (2×10^6 cells) in PBS were mixed with Matrigel (BD Biosciences). Matrigel (100 μl) and PBS (100 μl) were then mixed at a volume ratio of 1:1 and subcutaneously (s.c.) injected into the backs of athymic nude mice (groups 2, 3, 4, and 5). The volumes of JEG-3 tumor were measured daily using a caliper and calculated by width × length × height × 0.5236 (mm^3). To generate metastasis models, JEG-3 cells were prestained with CMFDA and detached using 0.05% trypsin-0.02% EDTA solution. JEG-3 cells (2×10^6 cells) in PBS were injected i.v. into the tail vein (groups 6, 7, and 8).

In Vivo Therapeutic Effect of Genetically Engineered hNSCs

To identify the inhibitory effects of genetically engineered hNSCs in mouse xenograft and metastasis models of choriocarcinoma, the mice were divided into eight experimental groups. Group 1 was an untreated negative control. Group 2 received only 5-FC (500 mg/kg/day) via intraperitoneal injection. In groups 3, 4, and 5, when the tumor mass reached 50 to 150 mm^3, animals were s.c. injected with CM-DiI prestained hNSCs (group 3, HB1.F3; groups 4, HB1.F3.CD; groups 5, HB1.F3.CD.IFN-β) in the presence of 5-FC. One week after intravenous injection of JEG-3, groups 6, 7, and 8 were i.v. injected with CM-DiI prestained hNSCs (group 6, HB1.F3; groups 7, HB1.F3.CD; groups 8, HB1.F3.CD.IFN-β) in the presence of 5-FC. This study was conducted for 21 days after the first hNSCs treatment. Animals were injected with hNSCs (2×10^6 cells) three times. Two days after the first treatment with hNSCs, 5-FC was intraperitoneally injected for 3 days in groups 2, 3, 4, 5, 6, 7, and 8. The effects of hNSCs on survival rate were measured for 50 to 60 days after the first JEG-3 injection. The mice were euthanized after 50 (Metastasis model) or 60 (Xenograft model) days of JEG-3 injection. After removing the tumors, lungs, uteruses, ovaries and spleens, the weights of organs were recorded and metastatic nodules were counted. Moreover, the metastatic area on the lung surface was measured using the Cell Sense Dimension software (Olympus), and graphs were drawn using Graphpad Prism (v5.0).

Ex Vivo Imaging

To confirm the migration ability of hNSCs *in vivo*, the lungs of mice injected into the tail vein with JEG-3 were analyzed. At 21 days after the first hNSCs injection, the mice were dissected and the lungs were obtained. CMFDA prestained JEG-3 and CM-DiI prestained hNSCs in groups 1, 6, 7, and 8 were then measured using a fluorescence *in vivo* imaging system (NEO Science).

In Vivo Fluorescence Analysis

To confirm the distribution of JEG-3 and hNSCs, cells were prestained with CMFDA or CM-DiI according to the manufacturer's protocols. Tissue sections of the lungs and tumors on the slides were then hydrated and fixed in 10% formalin, after which they were washed with PBS. After washing, the slides were treated with DAPI solution (600 nM) at room temperature, after which the tissue sections were mounted with cover glasses and confirmed using an IX-73 Inverted Microscope (Olympus).

Data Analysis

All experiments were conducted at least three times to demonstrate consistency of results. Statistical analyses of all results were performed using Graphpad Prism (v5.0; Graphpad software). Data are presented as the means ± standard error of the means. Two-way analysis of variance followed by *post hoc* Dunnett's or Tukey's multiple comparison tests for three-pair comparisons or Student's *t* tests for pairwise comparisons was used for data analysis. P values $< .05$ were considered statistically significant.

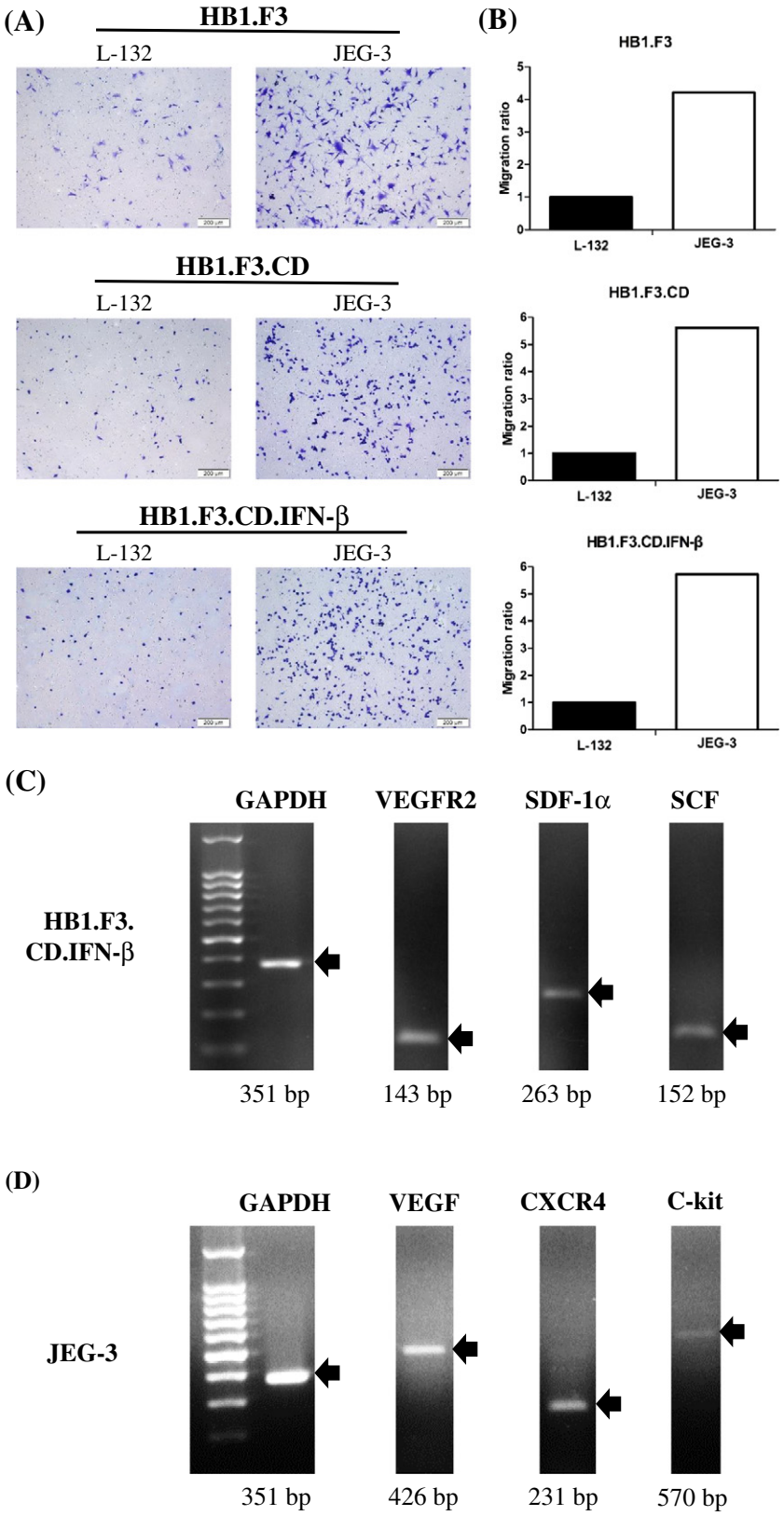

Figure 2. Migration ability of hNSCs to JEG-3 in response to chemoattractant factors. (A) L-132 (human pulmonary epithelial cells) and JEG-3 cells (1×10^5 cells/well) were seeded in the lower compartments of 24-well plates. hNSCs (1×10^5 cells/well) were also seeded in the fibronectin (20 μg/ml) precoated upper compartments. Crystal violet staining was performed to identify migrated cells. (B) The migration ratio of hNSCs was counted using the Cell Sense Dimension software. (C and D) Expression of chemoattractant factors in JEG-3 (C) and HB1.F3.CD.IFN-β cells (D) was confirmed by PCR.

Results

Ascertainment of Therapeutic Gene Expression in Genetically Engineered hNSCs

Expression of *E. coli* Cytosine deaminase (CD, 559 bp) and human Interferon-β (IFN-β, 296 bp) genes in HB1.F3.CD and HB1.F3.CD.IFN-β cells was ascertained by reverse transcription polymerase chain reaction (RT-PCR). HB1.F3.CD cells expressed the CD gene and HB1.F3.CD.IFN-β cells expressed the CD and IFN-β genes as shown in Figure 1. GAPDH (351 bp) was used as an internal control.

Specific Migration Ability of hNSCs Toward JEG-3 Cells

Migration of hNSCs was confirmed by migration assay. To measure the migrated hNSCs, Trans-well membranes were stained

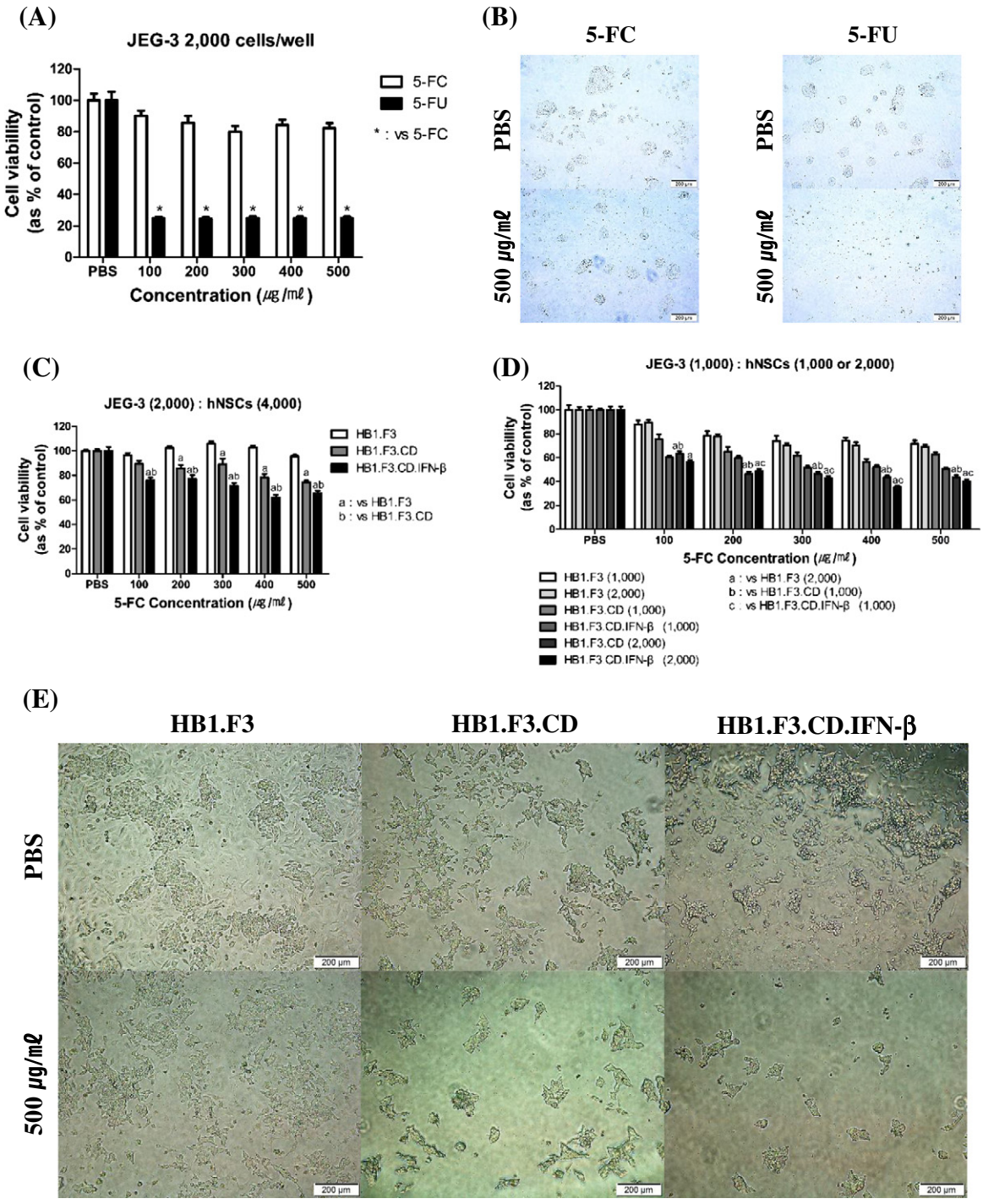

Figure 3. Inhibition of cell viability by genetically engineered hNSCs *in vitro*. (A) JEG-3 cells (2×10^3 cells / well) seeded on 96-well plates were treated with 5-FC or 5-FU for 3 days. (B) After 5-FC or 5-FU treatment for 3 days, microscopic analysis (×100) was performed. (C and D) JEG-3 (1×10^3 or 2×10^3 cells/well) and hNSCs (1×10^3, 2×10^3 or 4×10^3 cells/well) were co-cultured in 96-well plates and treated with 5-FC for 3 days. (E) Microscopic analysis (×100) after 5-FC treatment for 3 days. PBS was used as a negative control. Cell viability was confirmed by MTT solution assay. Data are presented as the means ± standard error of the mean. *$P < .05$ versus control.

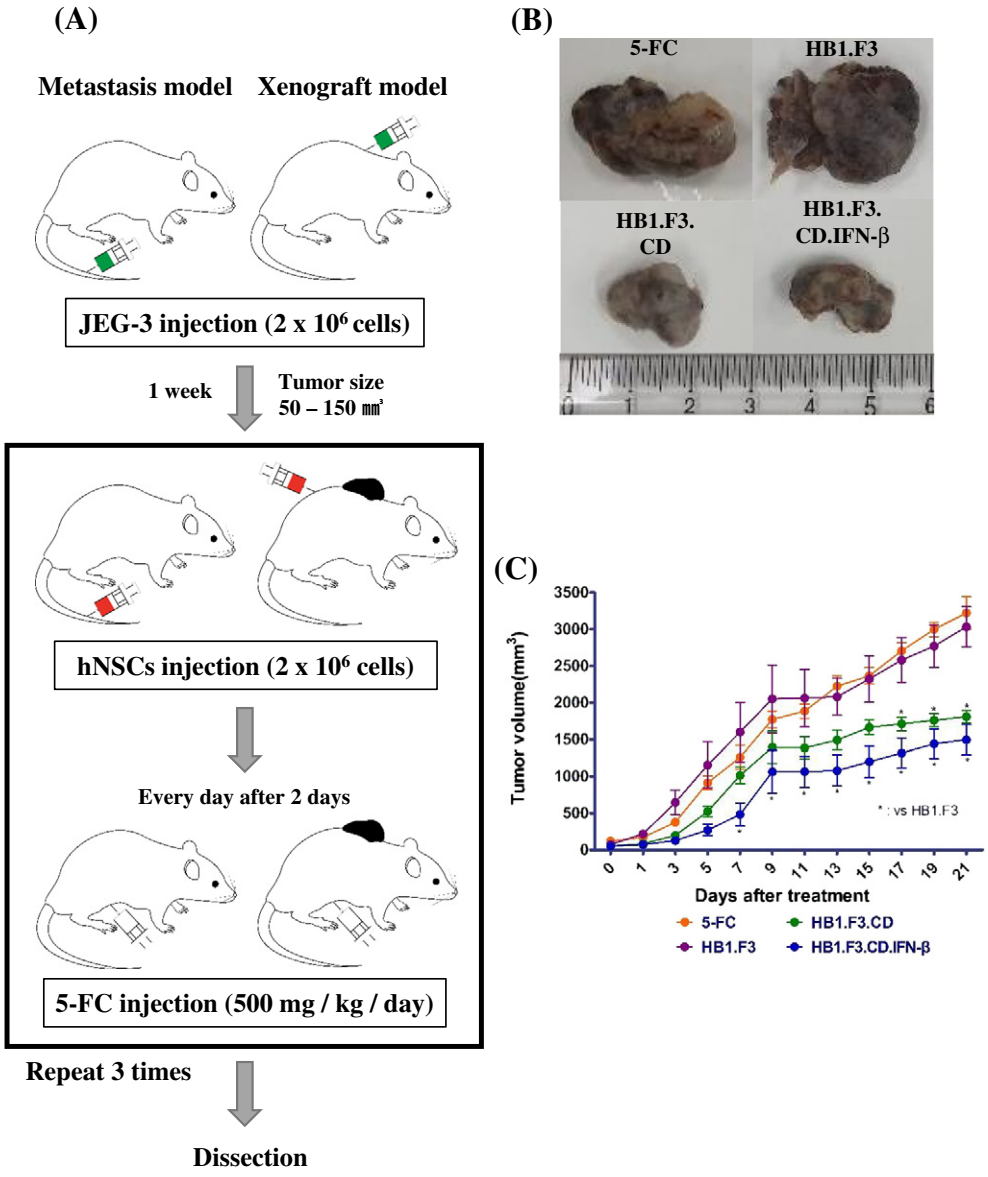

Figure 4. Inhibition of tumor growth by genetically engineered hNSCs treatment in a xenograft model. To establish xenograft and metastasis models, CMFDA prestained JEG-3 cells (2×10^6 cells) were s.c. and i.v. injected into female athymic nude mice. (A) One week after injection of JEG-3 cells, CM-DiI prestained hNSCs (2×10^6 cells) were i.v. injected into a metastasis model. When tumor masses reached 50 to 150 mm^3, CM-DiI prestained hNSCs (2×10^6 cells) were injected s.c. near the tumor mass in the xenograft model. After 2 days, 5-FC (500 mg/kg/day) was intraperitoneally injected every day. (B) Representative tumor images of JEG-3 cells xenografts. (C) Tumor volumes of the mice were measured with a caliper for 21 days. Data are presented as the means ± the standard error of the mean. *$P <$ .05 versus 5-FC treatment alone.

with crystal violet and observed under an IX-73 Inverted Microscope (Figure 2*A*). The number of hNSCs that migrated to JEG-3 or normal lung cells (L-132) was counted as a ratio using the Cell Sense Dimension software (Figure 2*B*). RT-PCR was performed to identify factors associated with cancer-specific migration. It is known that hNSCs have the capability to migrate toward cancer via chemoattractant factors. Therefore, expression of chemoattractant factors such as SCF, C-kit, SDF-1α, CXCR4, VEGF, and VEGFR2 was confirmed at the mRNA level. VEGFR2, SDF-1α, and SCF were expressed in HB1.F3.CD.IFN-β cells (Figure 2*C*), while VEGF, CXCR4, and C-kit were expressed in JEG-3 cells (Figure 2*D*). The same analysis was performed on L-132 cells. As a result, the expression of CXCR4 was confirmed, but the expression of VEGF and C-kit could not be confirmed in L-132 cells (data not shown).

Inhibitory Effects of CD and IFN-β Genes in the Presence of 5-FC

The inhibitory effects of 5-FC and 5-FU on choriocarcinoma were confirmed by MTT assay. The viability of JEG-3 cells was not affected by 5-FC treatment and was dramatically reduced by 5-FU treatment (Figure 3, *A* and *B*). hNSCs and JEG-3 were co-cultured with 5-FC to investigate the inhibitory effects of hNSCs expressing CD and IFN-β genes. The viability of JEG-3 cells was significantly decreased in the HB1.F3.CD and HB1.F3.CD.IFN-β groups, and the synergistic effects of CD and IFN-β genes were confirmed as seen in Figure 3, *C* and *E*. Moreover, the cell viability of JEG-3 decreased

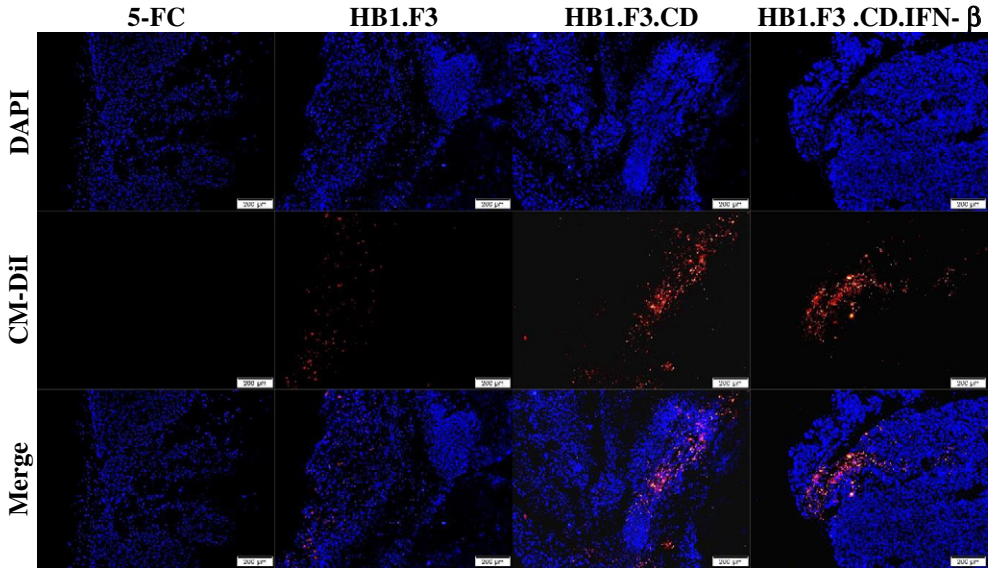

Figure 5. Fluorescence analysis of tumor sections extracted from s.c. injected mice. Tumors of mice injected with CM-DiI prestained hNSCs were harvested. Tumors were fixed in 10% formalin solution and sectioned with a microtome. After DAPI counterstaining, tumor sections were analyzed by fluorescence microscopy. DAPI (blue): nuclei of all cells, CM-DiI (red): hNSCs.

as the number of HB1.F3.CD and HB1.F.3.CD.IFN-β increased (Figure 3*D*).

Changes in Tumor Growth by Treatment of Genetically Engineered hNSCs

To confirm the anticancer effects of hNSCs, xenograft and metastasis models were established by the method shown in Figure 4*A*. During the experiment, the volume of the tumors was periodically measured with a caliper. In addition, the sizes of the extracted tumors were compared among groups. The growth of tumor volume was inhibited in the groups injected with HB1.F3.CD or HB1.F3.CD.IFN-β cells relative to the other groups (Figure 4, *B* and *C*). To investigate the tumor-specific migration of hNSCs *in vivo*, the extracted tumors were analyzed by fluorescence assay. CM-DiI prestained hNSCs were s.c. injected three times into the backs of the mice approximately 1 cm away from the tumor. Tumor sections of the mice were stained with DAPI staining solution, and fluorescence analysis was performed to confirm the presence of hNSCs in the tumor mass. Red fluorescence was detected in the tumor mass, indicating that the hNSCs had migrated toward the tumor (Figure 5). Red fluorescence was not observed in the 5-FC group, which received no hNSCs.

Inhibition of Lung Metastasis by Genetically Engineered hNSCs

To confirm the inhibitory effects of hNSCs expressing CD and IFN-β genes on lung metastasis of choriocarcinoma, the lungs of s.c. and i.v. injected mice were harvested. In the xenograft model, there was no visual difference in lung metastasis in response to hNSCs (s.c. injection) treatment as shown in Figure 6*B*. However, lung metastasis was suppressed in mice injected with HB1.F3.CD and HB1.F3.CD.IFN-β cells when compared to those injected with HB1.F3 cells in a metastasis (i.v. injection) model (Figure 6*A*). In the metastasis model, the metastatic region of the lung surface was decreased in the HB1.F3.CD group, with the HB1.F3.CD.IFN-β group showing particularly notable inhibition (Figure 6*C*). The weight of the lungs showed a similar pattern in metastasis model. Specifically, the weight of lungs from mice injected with JEG-3 was higher than that of normal mice, but the weight of those from the HB1.F3.CD.IFN-β group was close to that of normal mice (Figure 6*D*). Fluorescent signal intensity of prestained hNSCs (red CM-DiI) and JEG-3 (green CMFDA) cells in the lungs of mice fixed with 10% formalin was confirmed by *ex vivo* imaging. The signal intensity of CMFDA was decreased significantly in the HB1.F3.CD and HB1.F3.CD.IFN-β groups when compared to the HB1.F3 group, while there was no difference in the amount of CM-DiI expressed as demonstrated in Figure 6, *E* and *F*. Thus, all hNSCs showed the same migration capacity, and JEG-3 cells were reduced by the anticancer genes. Tissue slides were stained with DAPI solution for fluorescence analysis of lung sections of metastasis and xenograft models. The lungs of i.v. injected mice (metastasis model) were found to contain both hNSCs and JEG-3 cells, whereas hNSCs were not found in the lungs of s.c. injected mice (xenograft model) (Figure 7, *A* and *B*). These results indicated that s.c. injected hNSCs did not migrate to metastatic organs.

Effects of Genetically Engineered hNSCs on the Inhibition of Metastasis to Other Organs

We investigated the incidence of cancer in other organs (ovaries and uterus) associated with choriocarcinoma. The occurrence of cancer was confirmed in all groups except the negative control as shown in Figure 8, *A* and *B*. In the metastasis model, the ovarian weight of the HB1.F3 group was greatly increased by the tumor, but the HB1.F3.CD and HB1.F3.CD.IFN-β groups showed no significant change in ovary weight (Figure 8*C*). In addition, the number of ovarian metastatic nodules in the HB1.F3.CD and HB1.F3.CD.IFN-β groups of the xenograft model was reduced (Figure 8*D*). In the case of the uterus, uterine weight increased in all mice injected with JEG-3 cells when compared to the negative control (Figure 8, *E* and *F*). In the metastasis model, the weights of the HB1.F3.CD and HB1.F3.CD.IFN-β groups were lower than those of the HB1.F3 group. Spleen weight showed similar results as seen in Figure 9, *A* and *B*, while the weight of spleens of mice injected i.v. with HB1.F3.CD.IFN-β cells was similar to that of spleens from the negative control.

Extension of Survival Period by Treatment with Genetically Engineered hNSCs and 5-FC

Survival was confirmed for 50 to 60 days from the day of JEG-3 injection, which represented a significant prolongation in the groups treated with hNSCs expressing CD and/or the IFN-β genes as shown in Figure 10, *A* and *B*. However, there was no difference in survival between the HB1.F3.CD and HB1.F3.CD.IFN-β groups. Deaths associated with hNSCs and 5-FC treatment were not observed in any groups.

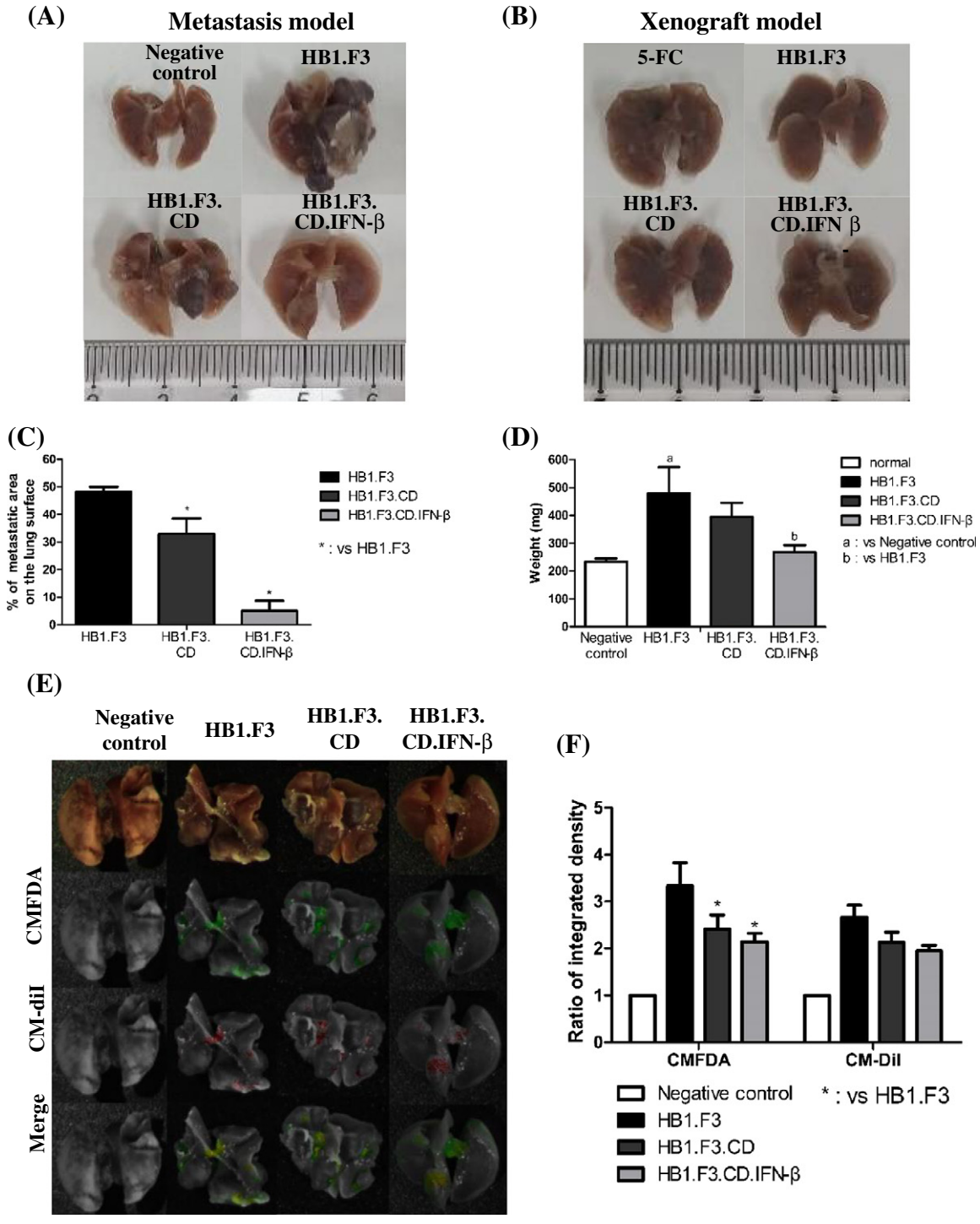

Figure 6. Inhibitory effect of hNSCs expressing therapeutic genes on lung metastasis in vivo. Representative lung images of metastasis (A) and xenograft models (B) are shown. (C) In the metastasis model, the metastatic area of the lung surface was measured using the Cell Sense Dimension software. (D) Lung weight of i.v. injected mice. (E**)** *Ex vivo* imaging of lungs from mice injected with JEG-3 cells and hNSCs i.v. CMFDA prestained JEG-3 cells and CM-DiI prestained hNSCs were injected. CMFDA (green): JEG-3 cells, CM-DiI (red): hNSCs. The lungs were imaged using a fluorescence imaging system. (F**)** The integrated density was measured in *ex vivo* images. The ratio of the integrated density was calculated based on the control group. The integrated density was calculated by the area × the mean intensity. Data are presented as the means ± the standard error of the mean. **P* < .05 versus HB1.F3.

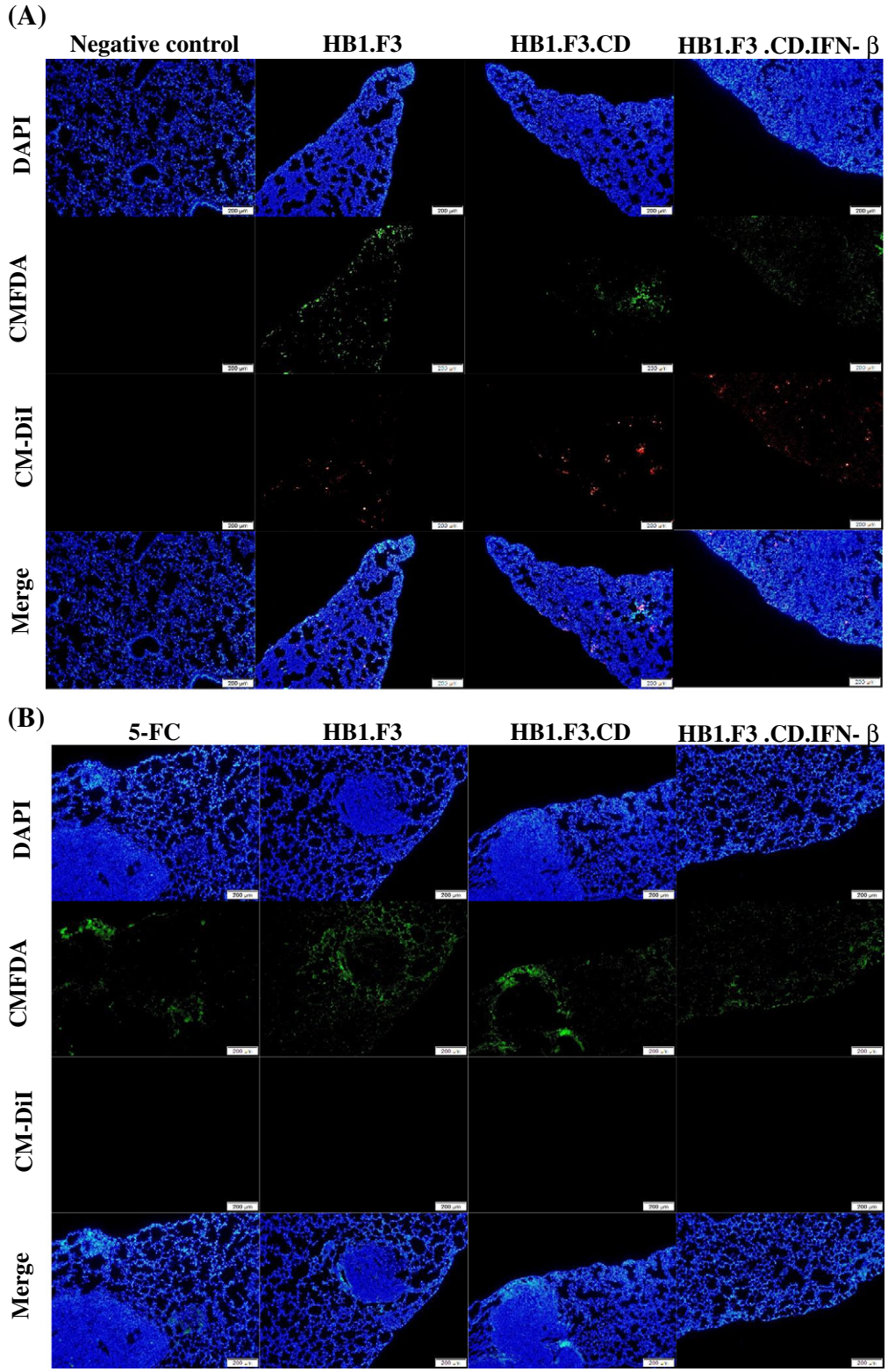

Figure 7. Migration of hNSCs in mouse metastasis model. CMFDA prestained JEG-3 cells and CM-DiI prestained hNSCs were injected i.v. or s.c. Lungs of the metastasis and xenograft models were extracted. Lungs were fixed with 10% formalin solution and sectioned using a microtome. After preparation of lung sections, DAPI counterstaining was performed. (A) Representative fluorescence analysis images of lung sections in metastasis model. (B) Detection of prestained cells (JEG-3 and hNSCs) in the lungs of xenograft model via fluorescence analysis. DAPI (blue): nuclei of all cells, CMFDA (green): JEG-3 cells, CM-DiI (red): hNSCs.

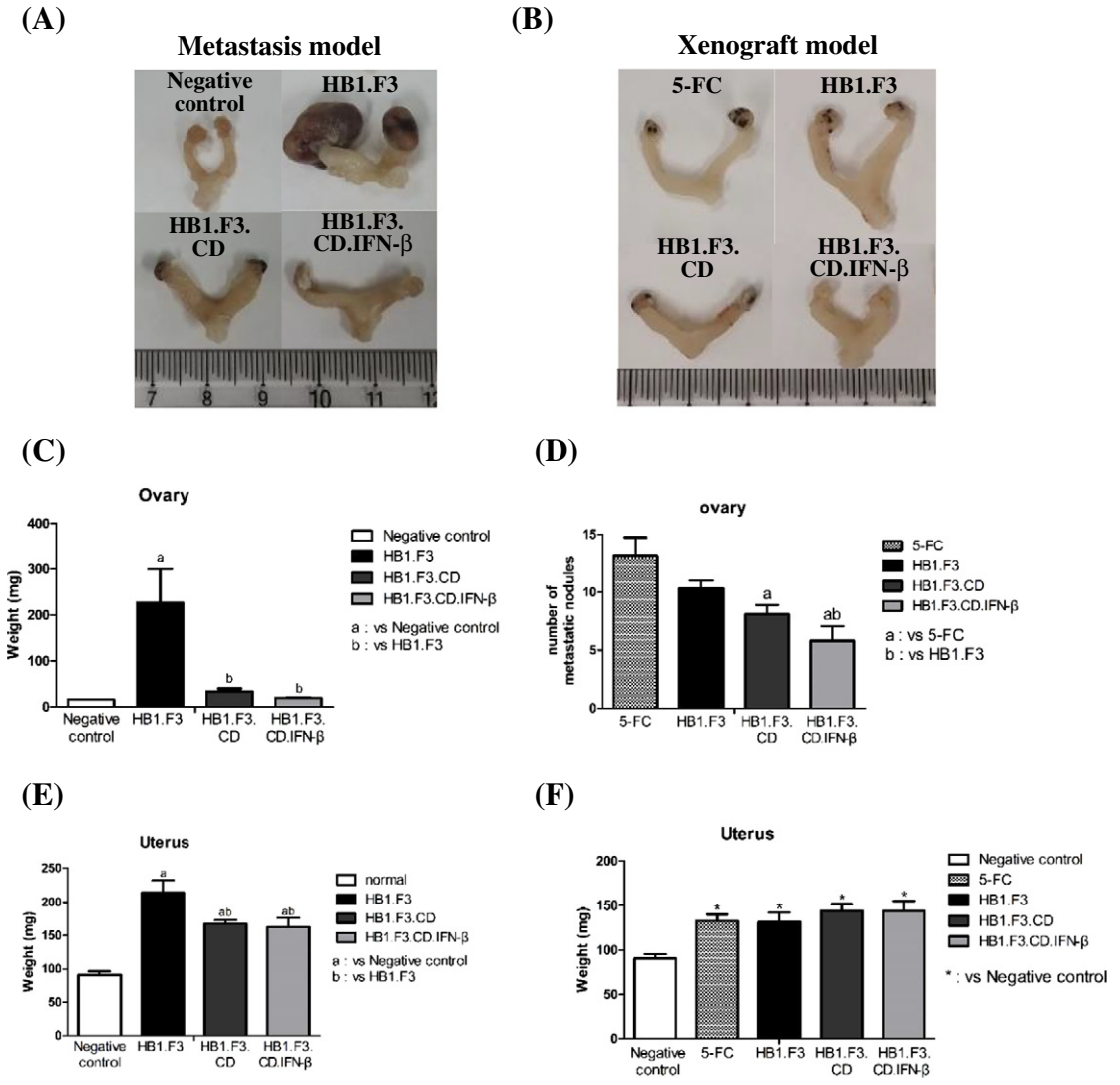

Figure 8. Changes in ovary and uterus in response to genetically engineered hNSCs treatment. (A and B) Representative images of ovaries and uterus in mouse metastasis and xenograft models. (C) Ovarian weight of mice injected i.v. (D) Quantification of lung metastatic nodules in i.v. injected mice. (E and F) Measurement of uterus weight in intravenous (E) and subcutaneous (F) injected mice. Data are presented as the means ± standard error of the mean. *$P < .05$ versus control.

Discussion

Choriocarcinoma is a highly invasive tumor with strong potential to metastasize to other organs. Choriocarcinoma is known to be capable of rapid metastasis through hematogenous pathways to multiple organs. Thus, when choriocarcinoma has metastasized to distant organs such as the lungs, treatment with conventional chemotherapy

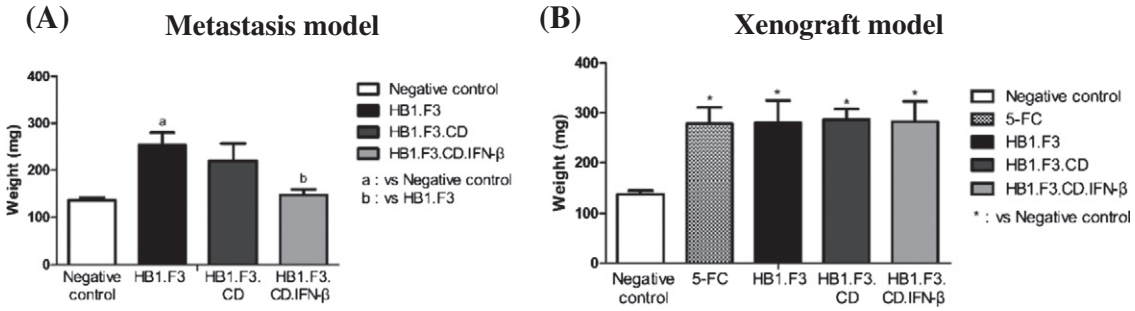

Figure 9. Measurement of spleen weight in mice injected with JEG-3 cells. After the mice were dissected, the spleens were weighed. (A) Change in spleen weight in response to genetically engineered hNSCs treatment in a metastasis model. (B) The weight of the spleen in mice injected s.c. Data are presented as the means ± the standard error of the mean. *$P < .05$ versus control.

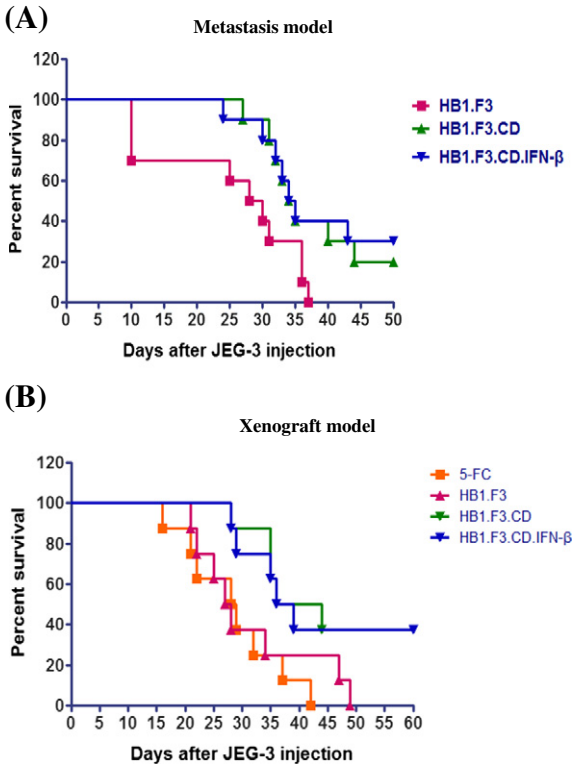

Figure 10. Changes in survival curve according to genetically engineered hNSCs treatment. On day 0, JEG-3 cells were injected into the tail vein (A) or the backs (B) of mice. Survival rates were continuously monitored after JEG-3 cells injection. The graph was calculated according to the following formula (current number of mice / initial number of mice × 100). Data are presented as the means ± the standard error of the mean ($P < .05$).

is difficult. Furthermore, anticancer drug resistance is an indisputable impediment to achieving definitive cancer treatment [1,32–34]. Consequently, it is necessary to identify novel treatments that can significantly improve the cure rate of metastatic choriocarcinoma.

In this study, we demonstrated the effects of GDEPT using neural stem cells for successful cancer treatment. Neural stem cells expressing anticancer genes were engineered by transduction with retrovirus. The tumor-tropic properties of these neural stem cells migrate to cancer cells. This was due to the interaction of neural stem cells with JEG-3 cancer cells that secrete chemoattractant factors such as VEGF, CXCR4, and C-kit [35–40]. In the migration assay, the number of neural stem cells migrating toward JEG-3 cells was about five times higher than that of normal human pulmonary epithelial cells (L-132) groups. Accordingly, cancer therapy using neural stem cells with migration capability has the potential to prevent damage to normal cells and minimize side effects.

The neural stem cells (HB1.F3.CD and HB1.F3.CD.IFN-β) used in this experiment were engineered to express CD and/or IFN-β. Pro-drug 5-FC is converted to the cytotoxic drug 5-FU by CD [41,42]. Previous studies have shown that GDEPT using neural stem cells exerted significant anticancer effects in various types of tumors [26–29]. The present study not only demonstrated synergistic effects of CD and IFN-β genes on choriocarcinoma but also confirmed that the viability of cancer cells was significantly reduced as the ratio of neural stem cells increased in co-culture systems.

In the mouse xenograft model, the therapeutic effects of hNSCs expressing the anticancer genes (CD and/or IFN-β) were confirmed against choriocarcinoma. Specifically, groups treated with HB1.F3.CD or HB1.F3.CD.IFN-β cells in the presence of 5-FC showed reductions in tumor volume by an average of about 50% when compared to the control groups (5-FC and HB1.F3 groups). However, there were no synergistic effects of CD and IFN-β genes on tumor volume.

Among the choriocarcinoma cell lines, JEG-3 cells are known to have stronger metastatic capability than JAR cells [30,43]. Accordingly, we injected JEG-3 cells and hNSCs into the tail veins of mice to establish a metastasis model. Tremendous lung metastasis was observed in the HB1.F3 group after termination of the experiment. However, a significant inhibitory effect was observed in the lungs of mice injected with hNSCs expressing the therapeutic genes. When compared with the HB1.F3 group, the HB1.F3.CD.IFN-β group showed an approximately 45% decrease in the metastatic area of the lung surface in the presence of 5-FC.

The migratory effect of hNSCs toward JEG-3 cells was confirmed in a xenograft model with metastasis. JEG-3 cells and three kinds of hNSCs were prestained with CMFDA and CM-DiI cell trackers, respectively, and then s.c. or i.v. injected into mice. Fluorescence analysis confirmed that hNSCs migrated to the tumors, indicating that hNSCs migrated through ligand-receptor interactions toward JEG-3 cells, which secrete chemoattractant factors. Fluorescence analysis of the lungs revealed metastasis in all JEG-3–injected mice groups. However, there were hNSCs in the lungs of the i.v. injected mice, while there were no hNSCs in mice that received subcutaneous injections. Meanwhile, it may be difficult to observe CMFDA-stained cancer cells and CM-DiI stained stem cells separately in the same lung tissues of the metastasis model due to possibility of signal overspill between the red and green fluorescence channels. However, it was detected that the signal intensity of CMFDA in the HB1.F3.CD and HB1.F.CD.IFN-β groups was significantly reduced compared to the HB1.F3 group despite the possibility of signal overspill between two fluorescences (Figure 6), indicating that i.v. injected hNSCs can more effectively target cancer cells that have metastasized to other organs. Furthermore, the survival rates of mice injected with hNSCs expressing the therapeutic genes increased significantly.

Comprehensively, the results of this study showed that HB1.F3.CD and HB1.F3.CD.IFN-β cells, which express CD and/or IFN-β genes, inhibit metastasis and suppress the viability of choriocarcinoma. Therapy with stem cells is expected to reduce side effects when compared to conventional chemotherapy because of its cancer-specific migration ability. In conclusion, the results of this study indicated that neural stem cells can be used as a noble vehicle to effectively target metastatic choriocarcinoma.

Acknowledgements

The authors appreciate Mr. Geon-Tae Park for technical supports for the experiments.

Funding Source

This work was supported by the Basic Science Research Program through the National Research Foundation of Korea (NRF) funded by the Ministry of Education, Science and Technology (MEST) (2016R1D1A1A09919809).

Conflicts of Interest Statement

The authors declare that there was no conflict of interest to be reported.

References

[1] Tian Q, Xue Y, Zheng W, Sun R, Ji W, Wang X, and An R (2015). Overexpression of hypoxia-inducible factor 1alpha induces migration and invasion through Notch signaling. *Int J Oncol* **47**(2), 728–738.

[2] Zhu Y, Yu M, Ma L, Xu H, and Li FR (2016). Choriocarcinoma-associated pulmonary thromboembolism and pulmonary hypertension: a case report. *J Biomed Res* **30**(3), 243–247.

[3] Guo J, Zhong C, Liu Q, Xu J, Zheng Y, Xu S, Gao Y, Guo Y, Wang Y, and Luo Q, et al (2013). Intracranial choriocarcinoma occurrence in males: two cases and a review of the literature. *Oncol Lett* **6**(5), 1329–1332.

[4] Ibi T, Hirai K, Bessho R, Kawamoto M, Koizumi K, and Shimizu K (2012). Choriocarcinoma of the lung: report of a case. *Gen Thorac Cardiovasc Surg* **60**(6), 377–380.

[5] Abbasi NZ, Zahur Z, Sheikh AS, Khan AA, Ahmed F, Memon KH, Ali F, Jeilani A, Fatima T, and Khan K, et al (2013). Testicular choriocarcinoma: diagnosed on cervical lymph node biopsy. *J Pak Med Assoc* **63**(12), 1544–1546.

[6] Tan Z, Zhang Y, Deng J, Zeng G, and Zhang Y (2012). Purified vitexin compound 1 suppresses tumor growth and induces cell apoptosis in a mouse model of human choriocarcinoma. *Int J Gynecol Cancer* **22**(3), 360–366.

[7] Chen Y, Qian H, Wang H, Zhang X, Fu M, Liang X, Ma Y, Zhan Q, Lin C, and Xiang Y (2007). Ad-PUMA sensitizes drug-resistant choriocarcinoma cells to chemotherapeutic agents. *Gynecol Oncol* **107**(3), 505–512.

[8] Nawa A, Tanino T, Luo C, Iwaki M, Kajiyama H, Shibata K, Yamamoto E, Ino K, Nishiyama Y, and Kikkawa F (2008). Gene directed enzyme prodrug therapy for ovarian cancer: could GDEPT become a promising treatment against ovarian cancer? *Anti Cancer Agents Med Chem* **8**(2), 232–239.

[9] Yi BR, Hwang KA, Aboody KS, Jeung EB, Kim SU, and Choi KC (2014). Selective antitumor effect of neural stem cells expressing cytosine deaminase and interferon-beta against ductal breast cancer cells in cellular and xenograft models. *Stem Cell Res* **12**(1), 36–48.

[10] Park GT and Choi KC (2016). Advanced new strategies for metastatic cancer treatment by therapeutic stem cells and oncolytic virotherapy. *Oncotarget* **7**(36), 58684–58695.

[11] Huber BE, Austin EA, Richards CA, Davis ST, and Good SS (1994). Metabolism of 5-fluorocytosine to 5-fluorouracil in human colorectal tumor cells transduced with the cytosine deaminase gene: significant antitumor effects when only a small percentage of tumor cells express cytosine deaminase. *Proc Natl Acad Sci U S A* **91**(17), 8302–8306.

[12] Kim KY, Kim SU, Leung PC, Jeung EB, and Choi KC (2010). Influence of the prodrugs 5-fluorocytosine and CPT-11 on ovarian cancer cells using genetically engineered stem cells: tumor-tropic potential and inhibition of ovarian cancer cell growth. *Cancer Sci* **101**(4), 955–962.

[13] Yi BR, Kim SU, and Choi KC (2016). Synergistic effect of therapeutic stem cells expressing cytosine deaminase and interferon-beta via apoptotic pathway in the metastatic mouse model of breast cancer. *Oncotarget* **7**(5), 5985–5999.

[14] Heo JR, Kim NH, Cho J, and Choi KC (2016). Current treatments for advanced melanoma and introduction of a promising novel gene therapy for melanoma (Review). *Oncol Rep* **36**(4), 1779–1786.

[15] Yi BR, Kang NH, Hwang KA, Kim SU, Jeung EB, and Choi KC (2011). Antitumor therapeutic effects of cytosine deaminase and interferon-beta against endometrial cancer cells using genetically engineered stem cells in vitro. *Anticancer Res* **31**(9), 2853–2861.

[16] Garrison JI, Berens ME, Shapiro JR, Treasurywala S, and Floyd-Smith G (1996). Interferon-beta inhibits proliferation and progression through S phase of the cell cycle in five glioma cell lines. *J Neuro-Oncol* **30**(3), 213–223.

[17] Ren C, Kumar S, Chanda D, Kallman L, Chen J, Mountz JD, and Ponnazhagan S (2008). Cancer gene therapy using mesenchymal stem cells expressing interferon-beta in a mouse prostate cancer lung metastasis model. *Gene Ther* **15**(21), 1446–1453.

[18] Yi BR, Kim SU, Kim YB, Lee HJ, Cho MH, and Choi KC (2012). Antitumor effects of genetically engineered stem cells expressing yeast cytosine deaminase in lung cancer brain metastases via their tumor-tropic properties. *Oncol Rep* **27**(6), 1823–1828.

[19] Kim SU, Jeung EB, Kim YB, Cho MH, and Choi KC (2011). Potential tumor-tropic effect of genetically engineered stem cells expressing suicide enzymes to selectively target invasive cancer in animal models. *Anticancer Res* **31**(4), 1249–1258.

[20] Jeong SW, Chu K, Jung KH, Kim SU, Kim M, and Roh JK (2003). Human neural stem cell transplantation promotes functional recovery in rats with experimental intracerebral hemorrhage. *Stroke* **34**(9), 2258–2263.

[21] Kim SU, Nakagawa E, Hatori K, Nagai A, Lee MA, and Bang JH (2002). Production of immortalized human neural crest stem cells. *Methods Mol Biol* **198**, 55–65.

[22] Kim YS, Hwang KA, Go RE, Kim CW, and Choi KC (2015). Gene therapy strategies using engineered stem cells for treating gynecologic and breast cancer patients (review). *Oncol Rep* **33**(5), 2107–2112.

[23] Yi BR, Hwang KA, Kang NH, Kim SU, Jeung EB, Kim HC, and Choi KC (2012). Synergistic effects of genetically engineered stem cells expressing cytosine deaminase and interferon-beta via their tumor tropism to selectively target human hepatocarcinoma cells. *Cancer Gene Ther* **19**(9), 644–651.

[24] Yi BR, Kim SU, and Choi KC (2015). Additional effects of engineered stem cells expressing a therapeutic gene and interferon-beta in a xenograft mouse model of endometrial cancer. *Int J Oncol* **47**(1), 171–178.

[25] Yi BR, Hwang KA, Kim YB, Kim SU, and Choi KC (2012). Effects of genetically engineered stem cells expressing cytosine deaminase and interferon-beta or carboxyl esterase on the growth of LNCaP rrostate cancer cells. *Int J Mol Sci* **13**(10), 12519–12532.

[26] Yi BR, O SN, Kang NH, Hwang KA, Kim SU, Jeung EB, Kim YB, Heo GJ, and Choi KC (2011). Genetically engineered stem cells expressing cytosine deaminase and interferon-beta migrate to human lung cancer cells and have potentially therapeutic anti-tumor effects. *Int J Oncol* **39**(4), 833–839.

[27] Park GT, Kim SU, and Choi KC (2017). Anti-proliferative effect of engineered neural stem cells expressing cytosine deaminase and interferon-beta against lymph node-derived metastatic colorectal adenocarcinoma in cellular and xenograft mouse models. *Cancer Res Treat* **49**(1), 79–91.

[28] Yi BR, Park MA, Lee HR, Kang NH, Choi KJ, Kim SU, and Choi KC (2013). Suppression of the growth of human colorectal cancer cells by therapeutic stem cells expressing cytosine deaminase and interferon-beta via their tumor-tropic effect in cellular and xenograft mouse models. *Mol Oncol* **7**(3), 543–554.

[29] Yi BR, Kim SU, and Choi KC (2014). Co-treatment with therapeutic neural stem cells expressing carboxyl esterase and CPT-11 inhibit growth of primary and metastatic lung cancers in mice. *Oncotarget* **5**(24), 12835–12848.

[30] Jingting C, Yangde Z, Yi Z, Huining L, Rong Y, and Yu Z (2007). Heparanase expression correlates with metastatic capability in human choriocarcinoma. *Gynecol Oncol* **107**(1), 22–29.

[31] Panngom K, Baik KY, Nam MK, Han JH, Rhim H, and Choi EH (2013). Preferential killing of human lung cancer cell lines with mitochondrial dysfunction by nonthermal dielectric barrier discharge plasma. *Cell Death Dis* **4**, e642.

[32] Kang KA and Hyun JW (2017). Oxidative stress, Nrf2, and epigenetic modification contribute to anticancer drug resistance. *Toxicol Res* **33**(1), 1–5.

[33] Denduluri SK, Wang Z, Yan Z, Wang J, Wei Q, Mohammed MK, Haydon RC, Luu HH, and He TC (2015). Molecular pathogenesis and therapeutic strategies of human osteosarcoma. *J Biomed Res* **30**(1), 5–18.

[34] Seckl MJ, Sebire NJ, and Berkowitz RS (2010). Gestational trophoblastic disease. *Lancet* **376**(9742), 717–729.

[35] Gupta N and Duda DG (2016). Role of stromal cell-derived factor 1alpha pathway in bone metastatic prostate cancer. *J Biomed Res* **30**(3), 181–185.

[36] Yi BR, Choi KJ, Kim SU, and Choi KC (2012). Therapeutic potential of stem cells expressing suicide genes that selectively target human breast cancer cells: evidence that they exert tumoricidal effects via tumor tropism (review). *Int J Oncol* **41**(3), 798–804.

[37] Lash GE, Warren AY, Underwood S, and Baker PN (2003). Vascular endothelial growth factor is a chemoattractant for trophoblast cells. *Placenta* **24**(5), 549–556.

[38] Zhang H, Vutskits L, Pepper MS, and Kiss JZ (2003). VEGF is a chemoattractant for FGF-2-stimulated neural progenitors. *J Cell Biol* **163**(6), 1375–1384.

[39] Koshiba T, Hosotani R, Miyamoto Y, Ida J, Tsuji S, Nakajima S, Kawaguchi M, Kobayashi H, Doi R, and Hori T, et al (2000). Expression of stromal cell-derived factor 1 and CXCR4 ligand receptor system in pancreatic cancer: a possible role for tumor progression. *Clin Cancer Res* **6**(9), 3530–3535.

[40] Kopparapu PK, Boorjian SA, Robinson BD, Downes M, Gudas LJ, Mongan NP, and Persson JL (2013). Expression of VEGF and its receptors VEGFR1/-VEGFR2 is associated with invasiveness of bladder cancer. *Anticancer Res* **33**(6), 2381–2390.

[41] Ye L, Tao K, Yu Y, and Wang G (2010). Reduction of G0 phase cells of colon cancer caco-2 cells may enhance 5-fluorouracil efficacy. *J Biomed Res* **24**(1), 64–68.

[42] Kim AY, Kwak JH, Je NK, Lee YH, and Jung YS (2015). Epithelial-mesenchymal transition is associated with acquired resistance to 5-fluorocuracil in HT-29 colon cancer cells. *Toxicol Res* **31**(2), 151–156.

[43] Grummer R, Hohn HP, Mareel MM, and Denker HW (1994). Adhesion and invasion of three human choriocarcinoma cell lines into human endometrium in a three-dimensional organ culture system. *Placenta* **15**(4), 411–429.